

1 Genetically identical twins show comparable tau PET load 2 and spatial distribution

3 Emma M. Coomans,^{1,2} Jori Tomassen,² Rik Ossenkoppele,^{2,3} Sandeep S. V. Golla,¹ Marijke den
4 Hollander,¹ Lyduine E. Collij,¹ Emma Weltings,¹ Sophie van der Landen,² Emma E. Wolters,¹
5 Albert D. Windhorst,¹ Frederik Barkhof,^{1,4} Eco J.C. de Geus,⁵ Philip Scheltens,² Pieter Jelle
6 Visser,^{2,6,7} Bart N. M. van Berckel¹ and Anouk den Braber^{2,5}

7 1 Department of Radiology & Nuclear Medicine, Amsterdam Neuroscience, Vrije Universiteit
8 Amsterdam, Amsterdam UMC, Amsterdam, The Netherlands

9 2 Alzheimer Center Amsterdam, Department of Neurology, Amsterdam Neuroscience, Vrije
10 Universiteit Amsterdam, Amsterdam UMC, Amsterdam, The Netherlands

11 3 Clinical Memory Research Unit, Lund University, Lund, Sweden

12 4 UCL Institute of Neurology, London, UK

13 5 Department of Biological Psychiatry, Vrije Universiteit Amsterdam, Amsterdam, The
14 Netherlands

15 6 Alzheimer Center Limburg, School for Mental Health and Neuroscience, Maastricht
16 University, Maastricht, The Netherlands

17 7 Department of Neurobiology, Care Sciences and Society, Division of Neurogeriatrics,
18 Karolinska Institutet, Stockholm Sweden

19 Correspondence to: Emma M. Coomans

20 Department of Radiology & Nuclear Medicine, Amsterdam UMC, VUmc

21 PO Box 7057, 1007MB Amsterdam, The Netherlands

22 E-mail: e.coomans@amsterdamumc.nl

23 **Running title:** Tau-PET in genetically identical twins

1 Abstract

2 Tau accumulation starts during the preclinical phase of Alzheimer's disease and is closely
3 associated with cognitive decline. For preventive purposes, it is important to identify factors
4 associated with tau accumulation and spread. Studying genetically identical twin-pairs may give
5 insight into genetic and environmental contributions to tau pathology, as similarities in identical
6 twin-pairs largely result from genetic factors, while differences in identical twin-pairs can largely
7 be attributed to non-shared, environmental factors. This study aimed to examine similarities and
8 dissimilarities in a cohort of genetically identical older twin-pairs in 1) tau load and 2) spatial
9 distribution of tau, measured with [¹⁸F]flortaucipir PET.

10 We selected 78 genetically identical twins (39 pairs; average age 73±6), enriched for
11 amyloid-β pathology and *APOE* ε4 carriership, who underwent dynamic [¹⁸F]flortaucipir PET.
12 We extracted binding potentials (BP_{ND}) in entorhinal, temporal, widespread neocortical and
13 global regions, and examined within-pair similarities in BP_{ND} using age and sex corrected intra-
14 class correlations. Furthermore, we tested whether twin-pairs showed a more similar spatial
15 [¹⁸F]flortaucipir distribution compared to non-twin pairs, and whether the participant's co-twin
16 could be identified solely based on the spatial [¹⁸F]flortaucipir distribution. Last, we explored
17 whether environmental (e.g. physical activity, obesity) factors could explain observed
18 differences in twins of a pair in [¹⁸F]flortaucipir BP_{ND}.

19 On visual inspection, Alzheimer's disease-like [¹⁸F]flortaucipir PET patterns were
20 observed, and although we mainly identified similarities in twin-pairs, some pairs showed strong
21 dissimilarities. [¹⁸F]flortaucipir BP_{ND} was correlated in twins in the entorhinal ($r=0.40$; $p=0.01$),
22 neocortical ($r=0.59$; $p<0.01$) and global ($r=0.56$; $p<0.01$) regions, but not in the temporal region
23 ($r=0.20$; $p=0.10$). The [¹⁸F]flortaucipir distribution pattern was significantly more similar
24 between twins of the same pair (mean $r=0.27$; $SD=0.09$) than between non-twin pairings of
25 participants (mean $r=0.01$; $SD=0.10$) ($p<0.01$), also after correcting for proxies of off-target
26 binding. Based on the spatial [¹⁸F]flortaucipir distribution, we could identify with an accuracy of
27 86% which twins belonged to the same pair. Finally, within-pair differences in [¹⁸F]flortaucipir
28 BP_{ND} were associated with within-pair differences in depressive symptoms ($0.37<\beta<0.56$),
29 physical activity ($-0.41<\beta<-0.42$) and social activity ($-0.32<\beta<-0.36$) (all $p<0.05$).

1 Overall, identical twin-pairs were comparable in tau load and spatial distribution,
2 highlighting the important role of genetic factors in the accumulation and spreading of tau
3 pathology. Considering also the presence of dissimilarities in tau pathology in identical twin-
4 pairs, our results additionally support a role for (potentially modifiable) environmental factors in
5 the onset of Alzheimer's disease pathological processes, which may be of interest for future
6 prevention strategies.

7 **Keywords:** Alzheimer's disease; tau; PET; twins; genetics

8 **Abbreviations:** BMI = body mass index; BP_{ND} = Binding Potential; DIN = Digit-in-Noise; GDS
9 = Geriatric Depression Scale; MAP = mean arterial pressure; MNI = Montreal Neurological
10 Institute; PASE = Physical Activity Scale for the Elderly; ROI = region-of-interest; SPM =
11 Statistical Parametric Mapping; SRT = speech reception threshold

12
13
14
15
16
17
18
19
20
21
22
23

ACCEPTED MANUSCRIPT

1 Introduction

2 The pathophysiological course of Alzheimer's disease lasts decades and includes a long
3 preclinical phase.¹ Within this preclinical phase, the brain gradually accumulates amyloid- β and
4 tau pathology, while cognitive functioning is still within normal limits.²⁻⁴ Whereas amyloid- β
5 plaques are detectable widespread throughout the brain relatively early in the disease course,⁵ the
6 distribution of neurofibrillary tau tangles starts focally and spreads throughout the brain followed
7 by clinical disease progression.^{6, 7} The neuropathological Braak staging system describes how
8 cortical neurofibrillary tau tangles are first observed in the (trans)entorhinal region of the medial
9 temporal lobe, followed by adjacent limbic and lateral temporal regions and finally the
10 neocortex.^{8, 9} This stereotypical tau spreading pattern has also been observed in *in vivo* positron
11 emission tomography (PET) studies at group-level,¹⁰⁻¹² although deviations from this pattern at
12 the individual-level may exist, including patterns of hemispheric asymmetry.^{7, 13} Studies have
13 shown that both the load and location of neurofibrillary tau tangles are closely associated with
14 cognitive functioning and decline.¹⁴⁻¹⁸ More specifically, the load of tau pathology correlates
15 with symptom severity or disease severity,¹⁶ and the regional localization of tau pathology
16 corresponds to the type of symptoms or disease phenotype.^{14, 19, 20} Also in cognitively
17 unimpaired elderly, subtle declines in cognitive functioning have been associated with tau
18 pathology in mainly medial temporal regions.^{15, 21-23} For preventive purposes, it is therefore
19 critical to understand which factors contribute to the accumulation onset and regional distribution
20 of tau pathology in the earliest stages of the disease.

21 Studying genetically identical twins provides an excellent approach to study the
22 contribution of genetic and environmental factors to a trait. As identical twin pairs share the
23 same genetic background, similarities in twins from a pair result from either shared genetic or
24 shared environmental factors, although the influence of shared environmental factors (e.g. being
25 raised in the same family) on brain measures in older twins is typically minimal.^{24, 25}
26 Dissimilarities in twins from a genetically identical pair will largely result from non-shared
27 environmental factors that are unique to one of the twins. Examining tau pathology in the
28 preclinical Alzheimer's disease phase in identical twins may thereby provide valuable
29 information for clinical trials aimed at prevention strategies.

30 The aim of this study is to assess to what extent genetic and environmental factors
31 contribute to tau pathology, as measured with [¹⁸F]flortaucipir PET, using a cohort of genetically

1 identical older twin pairs enriched for preclinical Alzheimer's disease pathology. In this study,
2 we assessed similarities in twins in two characteristics of tau PET: 1) tau load and 2) spatial
3 distribution of tau including hemispheric lateralization. Further, we explored which
4 environmental (e.g. physical activity, smoking or obesity) risk factors were associated with
5 observed differences in tau pathology, using a within twin-pair differences regression model. As
6 the heritability for Alzheimer's disease dementia is relatively high (i.e., genetic factors explain
7 up to 80% of the variance in Alzheimer's disease dementia)²⁶, and tau pathology is a key factor
8 in Alzheimer's disease, we hypothesize that large similarities in tau pathology in genetically
9 identical twins will be observed.

11 **Materials and methods**

12 **Participants**

13 We selected 80 genetically identical twins from the longitudinal Amsterdam sub-study of the
14 EMIF-AD PreclinAD cohort to undergo tau-PET imaging.²⁷ We selected twin-pairs of whom
15 both twins or either one of the twins were amyloid- β positive (based on baseline
16 [¹⁸F]flutemetamol PET visual read²⁸) or were classified into a high amyloid- β stage (based on a
17 previously applied staging model to the baseline [¹⁸F]flutemetamol PET scans²⁹), twin-pairs that
18 carried an *APOE* ϵ 4 allele, as well as age and sex matched amyloid- β negative twin-pairs. The
19 number of participants per amyloid- β stage are shown in **Supplementary Table 1**. Tau-PET was
20 performed during the EMIF-AD PreclinAD 4-year follow-up visit which took place 4.6 ± 0.6
21 years after the baseline visit. All participants had normal cognition at EMIF-AD PreclinAD study
22 enrolment. Baseline inclusion criteria were age ≥ 60 years, global Clinical Dementia Rating score
23 of 0, with a score of 0 on the memory sub domain,³⁰ delayed recall score > -1.5 SD of
24 demographics-adjusted normative data on the Consortium to Establish a Registry for
25 Alzheimer's Disease 10-word list,³¹ Telephone Interview for Cognitive Status modified score of
26 ≥ 23 , and a 15-item Geriatric Depression Scale score of < 11 .³² Baseline exclusion criteria were
27 any significant neurologic, systemic or psychiatric disorder that could cause cognitive
28 impairment. Additional exclusion criteria for tau-PET imaging were significant cerebrovascular
29 disease on MRI (e.g. territorial infarcts) or a history of major traumatic brain injury. Twin
30 zygosity was confirmed at baseline by buccal cell DNA analysis.

1 For the analyses, we only included complete twin pairs. Singletons (of which the co-twin
2 deceased prior to the 4-year follow-up visit and thus did not undergo tau-PET imaging, n=2
3 participants) were excluded, resulting in a total of 78 genetically identical twins (39 pairs)
4 included in the analyses.

5 The Medical Ethics Review Committee of the VU University Medical Center
6 (Amsterdam, The Netherlands) approved this study. All subjects provided written informed
7 consent.

8 **MRI acquisition**

9 Participants underwent three-dimensional T1 weighted MRI on a 3.0T Ingenuity TF PET/MR
10 (Philips Medical Systems, Best, The Netherlands). All MR scans were acquired within a
11 maximum of 12 months from the tau-PET scan (median time lag: 0.0 ± 5.9 months, IQR: 3.0
12 months).

13 **Tau-PET acquisition**

14 Participants underwent dual time-point dynamic [^{18}F]flortaucipir (tau) PET on an Ingenuity TF
15 PET/CT (Philips Medical Systems, Best, The Netherlands), which was validated in a previous
16 study.³³ [^{18}F]flortaucipir PET data were acquired during the 0-30min and 80-100min time
17 interval immediately following injection of 227 ± 56 MBq (injected mass 1.8 ± 1.2 μg). A low-
18 dose CT scan for attenuation correction was made prior to both the first and the second scan.
19 PET data were 3D RAMLA reconstructed with a matrix size of $128 \times 128 \times 90$ and a final voxel
20 size of $2 \times 2 \times 2$ mm³, and corrected for attenuation, scatter, randoms, decay and dead time.

21 **Tau-PET BP_{ND}**

22 Both parts of the dynamic scan were co-registered using Vinci software.³³ The high-resolution
23 T1 weighted MRI was co-registered to the corresponding PET images in native space using
24 Vinci software. Gray matter regions-of-interest (ROIs) from the Hammers template³⁴ and Svarer
25 template³⁵ were automatically delineated on the co-registered MR images and superimposed on
26 the PET scan using PVElab to extract time activity curves. Voxel-wise parametric images of
27 binding potential (BP_{ND}) were generated using receptor parametric mapping with whole
28 cerebellar gray matter from the Hammers template as the reference region.^{33, 36} PET images were
29 analysed with and without partial volume correction using Van Cittert iterative deconvolution

1 methods combined with highly constrained back-projection.³⁷ Results from partial volume
2 corrected data were similar and are shown in **Supplementary Table 2**.

3 **Tau-PET ROI analyses**

4 For ROI analyses, subject-space bilateral ROIs were a priori selected, in line with previous
5 studies and corresponding to Braak & Braak stages.^{8, 10, 38} We included the entorhinal cortex as
6 an early-stage tau region (Braak I) obtained from the Svarer template, as this region is not
7 available as a separate ROI in the Hammers template. We created a temporal composite ROI as
8 an intermediate-stage tau region (Braak III/IV), which included the amygdala, fusiform,
9 parahippocampal and ambient gyrus and middle and inferior temporal gyrus from the Hammers
10 template. We included a widespread neocortical composite ROI as a late-stage tau region (Braak
11 V/VI), which included the superior temporal gyrus, insula, lateral occipital lobe, cinguli anterior,
12 cinguli posterior, middle frontal, posterior temporal, inferolateral parietal, gyrus rectus,
13 orbitofrontal gyrus, inferior frontal gyrus, superior frontal, superior parietal, lingual gyrus,
14 cuneus, precentral and postcentral gyrus from the Hammers template. Last, a global brain region
15 was created including all ROIs from the early, intermediate and late tau stage regions combined
16 (i.e., Braak I-VI). The hippocampus was not included in the ROIs because of possible off-target
17 [¹⁸F]flortaucipir spill-in from the adjacent choroid plexus.³⁹

18 For each ROI, we also calculated a hemispheric lateralization measure (the laterality
19 quotient⁴⁰) using the formula $\text{Laterality quotient (\%)} = 100 \times (R - L) / (R + L)$.¹⁴ This
20 quotient was used to examine how similar twins were in lateralized (asymmetric)
21 [¹⁸F]flortaucipir uptake, as a measure for spatial distribution. A negative laterality quotient
22 indicates more tau in the left hemisphere, while a positive laterality quotient indicates more tau
23 in the right hemisphere.

24 **Tau-PET voxel-wise analyses**

25 For voxel-wise analyses, we spatially normalized the parametric PET images to Montreal
26 Neurological Institute (MNI) space using Statistical Parametric Mapping (SPM) version 8
27 software (Wellcome Trust Center for Neuroimaging, University College London, UK) by using
28 the transformation matrixes derived from warping the co-registered T1 weighted MRI scans to
29 MNI space. All warped images were visually checked for transformation errors. We created a
30 group-average image of [¹⁸F]flortaucipir BP_{ND} for visualisation purposes. Prior to voxel-wise

1 statistical analyses, a cerebral gray matter mask (excluding the basal ganglia because of potential
2 off-target [^{18}F]flortaucipir binding) was applied to the MNI-transformed images. These images
3 were used to assess within-pair similarities in voxel-by-voxel [^{18}F]flortaucipir spatial
4 distribution.

6 **Amyloid- β PET visual read and global BP_{ND}**

7 Participants underwent dynamic [^{18}F]flutemetamol (amyloid- β) PET during the EMIF-AD
8 PreclinAD baseline visit (i.e. 4 years prior to tau-PET) as previously described^{28, 41}. For
9 stratification analyses, we used baseline amyloid- β status (positive/negative) based on majority
10 visual read of the dynamic [^{18}F]flutemetamol BP_{ND} images.²⁸ Baseline [^{18}F]flutemetamol BP_{ND}
11 visual read was missing for three participants, for which we used baseline [^{18}F]flutemetamol
12 SUVr visual read (n=2) or [^{18}F]flutemetamol SUVr visual read obtained at time of tau-PET
13 (n=1). Global baseline [^{18}F]flutemetamol BP_{ND} , calculated as previously described,⁴¹ was used as
14 a covariate in further exploratory statistical analyses (missing for n=4 participants).

15 **Environmental risk factors**

16 As differences in identical twin pairs can largely be attributed to non-shared environmental (e.g.
17 physical activity and smoking) factors, we exploratory examined whether within-pair differences
18 in [^{18}F]flortaucipir BP_{ND} were associated with within-pair differences in environmental factors. In
19 line with the Lancet Commission 2020 update on dementia prevention, intervention, and care on
20 potentially modifiable risk factors for late-life cognitive decline,⁴² we included proxy variables
21 for 1) less education (years of education); 2) hearing loss (speech reception threshold (SRT) on
22 the Digit-in-Noise (DIN) test,⁴³ measuring auditory speech recognition abilities in noise); 3)
23 hypertension (average mean arterial pressure (MAP) from three subsequent measurements); 4)
24 alcohol (current number of glasses consumed per day); 5) obesity (body mass index (BMI)); 6)
25 smoking (number of pack years); 7) depression (Geriatric Depression Scale (GDS) total score)³²;
26 8) social isolation (The Health Related Quality of Life Short Form 12 sub-question: “Did your
27 health limited your social activities?”); and 9) physical inactivity (Physical Activity Scale for the
28 Elderly (PASE) total score)⁴⁴. Risk factor variables were assessed within the EMIF-AD
29 PreclinAD study at time of tau-PET imaging. Although listed as potentially modifiable risk
30 factors,⁴² we did not include traumatic brain injury (due to it being an exclusion criteria in the

1 current study), air pollution and diabetes (no suitable measures available). Details regarding
2 these questionnaires and measurements are specified in **Supplementary Table 3**.

3 **Statistical analyses**

4 All statistical analyses were performed in R (R, version 3.6.1, [www://R-project.org](http://www.R-project.org)). A p -value <
5 0.05 was considered statistically significant.

6 ***Similarities in twins in [^{18}F]flortaucipir BP_{ND}***

7 To examine similarities in twins in [^{18}F]flortaucipir BP_{ND} (tau load), we performed one-way
8 single-measure intra-class correlations across twin pairs for each ROI (i.e. a correlation between
9 Twin 1 and Twin 2 across the group) (**Fig. 3A**). Because identical twins share the same genetic
10 background, these intra-class correlations provide an estimate of the upper limit of genetic
11 contribution to a trait. We repeated these correlation analyses for 20 different sets (each set
12 consisting of 39 pairs) of random (non-twin) pairs using Pearson correlations. We then
13 determined whether the twin pair correlation coefficient was significantly higher than the
14 average correlation coefficient observed for random pairs using the Fisher-Z-transformation and
15 z -test statistic. This reflects whether twin-pairs are more similar in tau load than what would be
16 observed by chance (i.e. in randomly paired participants). Both the twin pair correlation analyses
17 and the random pair correlation analyses were adjusted for age and sex. We explored the effect
18 of baseline amyloid- β status on the within-pair similarities in [^{18}F]flortaucipir BP_{ND} by stratifying
19 the sample based on twins concordant on amyloid- β status (i.e. both twins of the same pair
20 amyloid- β negative or both twins of the same pair amyloid- β positive) and twins discordant on
21 amyloid- β status (i.e. one twin of the same pair amyloid- β negative and the co-twin amyloid- β
22 positive).

23 ***Similarities in twins in spatial distribution of [^{18}F]flortaucipir BP_{ND}***

24 We examined similarities in spatial distribution of [^{18}F]flortaucipir BP_{ND} in twins using three
25 different approaches (all adjusted for age and sex). First, we assessed within-pair similarities in
26 regional hemispheric laterality quotients for [^{18}F]flortaucipir BP_{ND} by performing one-way
27 single-measure intra-class correlations across twin pairs. This reflects whether twins show
28 similar hemispheric lateralization patterns of [^{18}F]flortaucipir BP_{ND} .

29 Second, for every participant, we extracted [^{18}F]flortaucipir BP_{ND} in each voxel from the
30 MNI-space images with a GM mask overlaid. We correlated each participant's voxel-by-voxel

1 [¹⁸F]flortaucipir spatial distribution to that of every other participant using Spearman correlation
 2 models (**Fig. 5A**). This yielded 77 correlation coefficients for every participant (resulting in a
 3 78x78 matrix of correlation coefficients) indicating how similar a participant's [¹⁸F]flortaucipir
 4 spatial distribution is to that of every other participant. An independent t-test was performed to
 5 assess whether the average correlation coefficient obtained for twin pairs was significantly
 6 higher than the average correlation coefficient obtained for non-twin pairings of participants.
 7 This yields an estimate of whether twin pairs show a more similar [¹⁸F]flortaucipir spatial
 8 distribution than non-twin pairs. To ensure that within-pair similarities in spatial distribution
 9 could not solely be explained by similarities in MNI-space warping parameters, we repeated the
 10 analysis with subject-space brain regions from the Hammers template (including the same
 11 regions as included in the Braak III-IV and Braak V-VI ROIs).

12 Last, we assessed whether we could successfully identify a participant's co-twin based on
 13 the strength of the previously established spatial correlation. If the highest correlation was
 14 observed for a participant's co-twin (instead of for a random other participant), it was considered
 15 a match. Otherwise, it was considered a miss. The success rate for twin pair identification was
 16 defined as the ratio between the number of matches and the total number of participants
 17 ($success\ rate\ (\%) = \frac{\#\ matches}{\#\ participants} * 100$).

18 As previous studies have postulated that cortical [¹⁸F]flortaucipir signal in cognitively
 19 unimpaired elderly may be affected by off-target binding,⁴⁵ we performed sensitivity analyses in
 20 which we, for each cortical voxel, regressed out part of the signal that could be explained by off-
 21 target binding in the thalamus and putamen⁴⁵ using SPM12, to ensure that these results could not
 22 solely be explained by within-pair similarities in off-target binding.

23
 24 ***Within twin-pair differences in BP_{ND} vs. within twin-pair differences in***
 25 ***environmental risk factors***

26 We explored whether within-pair differences in [¹⁸F]flortaucipir BP_{ND} were associated with
 27 within-pair differences in environmental risk factors using the within-identical twin pair
 28 difference model.⁴⁶ Specifically, we regressed the difference in regional [¹⁸F]flortaucipir BP_{ND} in
 29 identical twin pairs on the difference in environmental risk factors in the same pair of twins
 30 corrected for age and sex. In a separate model, we additionally corrected for within-pair

1 differences in global [^{18}F]flutemetamol BP_{ND} to explore whether observed associations were
2 explained by within-pair differences in global amyloid- β load. Within-pair difference models
3 with the DIN SRT score, a measure of hearing ability, were additionally corrected for hearing
4 aid.

5 **Data availability**

6 The data that support the findings of this study are available from the corresponding author, upon
7 reasonable request.

8 **Results**

9 Demographic characteristics and [^{18}F]flortaucipir BP_{ND} in each ROI are summarized in **Table 1**.
10 Seventy-eight participants (39 twin pairs) with an age of 73.4 ± 5.9 years were included in the
11 analyses. Of the 78 participants, 40 (51.3%) carried an *APOE* $\epsilon 4$ allele and 15 (19.2%) were
12 visually assessed as amyloid- β positive (4 years prior to tau-PET).
13

14 Mean [^{18}F]flortaucipir BP_{ND} was highest in the temporal (Braak III-IV) ROI (**Table 1**).
15 This was also observed in the group-average image of [^{18}F]flortaucipir BP_{ND} , revealing a
16 predominant temporal binding pattern (**Fig. 1**). High [^{18}F]flortaucipir BP_{ND} was also observed in
17 regions in the basal ganglia, typically known to be affected by off-target [^{18}F]flortaucipir
18 binding.

19 **Visual inspection of [^{18}F]flortaucipir PET**

20 On visual inspection, we mostly observed similarities in twins in both the intensity as well as the
21 distribution of [^{18}F]flortaucipir binding. However, dissimilarities in twins in [^{18}F]flortaucipir
22 PET were also observed. **Fig. 2** shows [^{18}F]flortaucipir PET scans from four identical twin pairs
23 showing similarities and two pairs showing dissimilarities in [^{18}F]flortaucipir PET, that were
24 selected for illustration purposes.

25 **Twin pair similarities in global and regional [^{18}F]flortaucipir BP_{ND}**

26 In twins (corrected for effects of age and sex), global (Braak I-VI) [^{18}F]flortaucipir BP_{ND}
27 correlated significantly ($r = 0.56$; $p < 0.01$) (**Fig. 3B**). Regionally, [^{18}F]flortaucipir BP_{ND}
28 moderately correlated in twins in the entorhinal (Braak I) ($r = 0.40$; $p = 0.01$) and neocortical
29 composite (Braak V-VI) ($r = 0.59$; $p < 0.01$) regions (**Fig. 3B**). The within-pair correlation for
30 [^{18}F]flortaucipir BP_{ND} in the temporal composite (Braak III-IV) region, however, was non-

1 significant ($r = 0.20$; $p = 0.10$) and fell within the range of what was found for random pairs
2 (**Fig. 3B and 3C**). The correlation coefficient observed for twin pairs was significantly higher
3 than the average correlation coefficient observed for random pairs for the entorhinal (r twin
4 pairs: 0.40 vs. average r random pairs: 0.01), neocortical composite (r twin pairs: 0.59 vs.
5 average r random pairs: 0.00) and global (r twin pairs: 0.56 vs. average r random pairs: 0.01)
6 regions, but not for the temporal composite region (r twin pairs: 0.20 vs. average r random pairs:
7 0.06) (**Fig. 3C**).

8 We next explored the influence of baseline amyloid- β status on the observed within-pair
9 correlations for [^{18}F]flortaucipir BP_{ND} . We observed that twin-pairs discordant on amyloid- β
10 status 4 years prior to tau-PET (i.e. one twin being amyloid- β positive and the co-twin amyloid- β
11 negative) often acted as outliers in the scatterplots (**Fig. 3B**). We therefore repeated the within-
12 pair correlations after stratifying the sample based on discordant amyloid- β status ($n=7$ pairs) or
13 concordant amyloid- β status ($n=32$ pairs). In amyloid- β concordant twins (corrected for effects
14 of age and sex), [^{18}F]flortaucipir BP_{ND} was moderate-to-strongly correlated in all ROIs, with
15 strongest correlations observed in the neocortical composite ($r = 0.77$; $p < 0.01$) and global ($r =$
16 0.75 ; $p < 0.01$) regions, followed by the temporal composite ($r = 0.33$; $p = 0.03$) and entorhinal (r
17 $= 0.48$; $p < 0.01$) regions (**Supplementary Table 4**). In contrast, in amyloid- β discordant twins,
18 [^{18}F]flortaucipir BP_{ND} was not significantly correlated in any of the ROIs (range r : 0.04-0.25;
19 range p : 0.26-0.45) (**Supplementary Table 4**).

20 **Twin pair similarities in spatial distribution of [^{18}F]flortaucipir** 21 **BP_{ND}**

22 Next, we examined similarities in identical twin pairs in the spatial distribution of
23 [^{18}F]flortaucipir BP_{ND} . First, within-pair similarities in spatial distribution were examined
24 regionally with the laterality quotient. Hemispheric lateralization in regional [^{18}F]flortaucipir
25 BP_{ND} was significantly correlated in twins in the temporal ($r = 0.58$; $p < 0.01$), neocortical ($r =$
26 0.69 ; $p < 0.01$) and global ($r = 0.69$; $p < 0.01$) regions. No correlation in twins was observed in
27 entorhinal hemispheric lateralization of [^{18}F]flortaucipir ($r = 0.09$; $p = 0.28$) (**Fig. 4**).

28 Second, we correlated each participant's voxel-by-voxel [^{18}F]flortaucipir spatial
29 distribution to that of every other participant (**Fig. 5A**). Correlations of [^{18}F]flortaucipir BP_{ND}
30 across voxels were on average significantly higher for twin pairs (mean $r = 0.27$; $SD = 0.09$) than

1 for non-twin pairings (mean $r = -0.01$; $SD = 0.10$) ($p < 0.01$) (**Fig. 5B**). These results were not
2 affected when correcting for proxies of cortical off-target binding (mean r for twin pairs: $0.27 \pm$
3 0.09 vs. mean r for non-twin pairs: -0.01 ± 0.09) ($p < 0.01$) or when correlating [^{18}F]flortaucipir
4 BP_{ND} across subject-space ROIs instead of MNI-space voxels (mean r for twin pairs: 0.57 ± 0.23
5 vs. mean r for non-twin pairs: -0.01 ± 0.33) ($p < 0.01$).

6 Last, based on the strength of the spatial voxel-wise correlation between participants, we
7 assessed the success rate in identifying a participant's co-twin. For 85.9% of the subjects, the
8 highest spatial correlation was observed for a participant's co-twin instead of for a random other
9 participant ($67/78 = 85.9\%$). Upon adjusting for proxies of cortical off-target binding, the success
10 rate remained high at 83.3%.

11 **Environmental risk factors associated with within-pair differences** 12 **in BP_{ND}**

13 As we also observed differences in twins in [^{18}F]flortaucipir PET (**Fig. 2**), which can largely be
14 attributed to non-shared, environmental (e.g. lifestyle) factors, we explored whether within-pair
15 differences in global and regional [^{18}F]flortaucipir BP_{ND} were associated with within-pair
16 differences in environmental risk factors. Corrected for age and sex, within-pair differences in
17 [^{18}F]flortaucipir BP_{ND} were associated with within-pair differences in GDS total score
18 ($0.37 < \beta < 0.56$; $p < 0.05$, depending on the ROI), within-pair differences in social activity ($-$
19 $0.32 < \beta < -0.36$; $p < 0.05$, depending on the ROI) and within-pair differences in PASE total score
20 ($-0.41 < \beta < -0.42$; $p < 0.05$ depending on the ROI) (**Fig. 6 and Supplementary Table 5**).
21 Specifically, the twin with a higher [^{18}F]flortaucipir BP_{ND} also had more depressive symptoms,
22 more strongly affected social activity and less physical activity. Upon additionally correcting the
23 within-pair difference regression models for within-pair differences in global [^{18}F]flutemetamol
24 BP_{ND} , within-pair differences in entorhinal [^{18}F]flortaucipir BP_{ND} remained associated with
25 within-pair differences in GDS total score ($\beta = 0.39$; $p = 0.02$), and within-pair differences in
26 entorhinal and temporal [^{18}F]flortaucipir BP_{ND} remained associated with within-pair differences
27 in PASE total score ($\beta = 0.40$; $p = 0.01$ and $\beta = 0.33$; $p = 0.02$, respectively). Effect sizes and
28 corresponding p -values are shown in **Supplementary Table 5**.

29

30

1 Discussion

2 In this study, we examined similarities and dissimilarities in genetically identical cognitively
3 unimpaired older twins in load and spatial distribution of tau pathology measured with
4 [¹⁸F]flortaucipir PET. We observed substantial within-pair similarities in tau pathology load,
5 voxel-wise spatial distribution and asymmetry measures. Based on the spatial distribution of tau
6 pathology, we could identify which twins belonged to the same pair with an accuracy of 86%.
7 These results suggest genetic factors to play an important role in the earliest increases and spatial
8 patterns of tau pathology. However, dissimilarities in twins in tau PET were also observed,
9 indicating a potential role for (possibly modifiable) environmental factors in secondary
10 prevention.

11 One of the main findings in the present study was that global and regional tau PET load
12 were significantly correlated in twins, and twins of the same twin pair were significantly more
13 alike in their tau PET load than random paired twin individuals, also after adjusting for potential
14 age- and sex-effects. This is in line with our earlier study,⁴¹ in which we observed within-pair
15 similarities in cerebrospinal fluid tau pathology of similar strength as to what we currently
16 observed using PET imaging. Observations from post-mortem human brains of monozygotic
17 twins with and without diagnosis of clinical Alzheimer's disease dementia have indicated both
18 within-pair concordances⁴⁷ as well as within-pair discordances⁴⁸ in neurofibrillary tau tangle
19 Braak staging. These results suggest that the susceptibility to and initial development of
20 pathology may be genetically determined, but genetics alone may not be sufficient to determine
21 the complete pathological and clinical course of the disease.

22 We observed moderate-to-strong within-pair correlations for regional tau pathology in the
23 entorhinal and neocortical composite region, but a substantial weaker and non-significant
24 correlation in the temporal composite region. The moderate within-pair correlation in the
25 entorhinal cortex, one of the brain sites in the medial temporal lobe in which neurofibrillary
26 tangles appear first,^{8, 9} suggests genetic factors to influence the earliest increases of tau
27 pathology. Tau tangles in the medial temporal lobe in cognitively unimpaired individuals have
28 previously been associated with subtle cognitive deficits and longitudinal cognitive decline^{15, 21-23}
29 , even when tau-tracer binding is lower than observed in clinical Alzheimer's disease, and
30 therefore do not seem to be benign. Whether or not a genetic predisposition to the earliest
31 increases in entorhinal tau translates to a risk for future clinical progression needs further

1 investigation. The within-pair correlation in the temporal composite region (Braak III-IV) was
2 affected by some twin pairs acting as outliers in the analysis. Interestingly, upon further
3 inspection, we noted that the twin pairs that acted as outliers – and thus were dissimilar in their
4 temporal tau-PET BP_{ND} – were often also discordant on their baseline amyloid- β status, meaning
5 one twin being amyloid- β positive and the co-twin being amyloid- β negative based on PET
6 visual read. Repeating the analysis while excluding the amyloid- β discordant twin pairs indeed
7 led to a strengthening of the within-pair correlation in temporal BP_{ND} . Studies have indicated that
8 tau pathology beyond the medial temporal lobe is typically accompanied with the presence of
9 cortical amyloid- β pathology,⁴⁹ which has led to the hypothesis that amyloid- β plays a key factor
10 in the spread of tau outside of the medial temporal lobe. Our results are in line with this
11 hypothesis, as within-pair similarities in twins in the temporal composite region (including
12 lateral temporal regions) became stronger and significant when amyloid- β discordant twins were
13 excluded, although it is notable that the within-pair correlation in the temporal region remained
14 considerably weaker than that of the other brain regions, suggesting a role for other factors (or
15 mechanisms) as well. Following the same hypothesis, it would have been expected that this
16 would also affect the within-pair correlation in neocortical tau pathology. Instead, we observed a
17 strong within-pair correlation for neocortical tau, exceeding levels of similarity that could have
18 been obtained by chance. However, cautious interpretation is needed for the within-pair
19 correlation in neocortical tau, as the BP_{ND} are all in the very low range. A cohort also consisting
20 of twin pairs with clinically manifest Alzheimer's disease might be preferred to infer conclusions
21 on similarities in tau pathology in late-stage tau.

22 Our data suggests that not only early tau load is under genetic influence, but also the
23 regional localization of tau. Although the amount of preclinical Alzheimer's disease tau
24 pathology is overall low (for comparison, in the current study we observed a Braak III-IV BP_{ND}
25 of 0.1 ± 0.1 , whereas we previously observed a BP_{ND} of 0.4 ± 0.2 in clinical Alzheimer's disease⁵⁰),
26 we observed strong similarities in pairs in asymmetric deposition of tau within larger cortical
27 regions. Asymmetric tau deposition is a characteristic feature in atypical Alzheimer's disease
28 phenotypes, but some degree of lateralization also exists in typical Alzheimer's disease.^{7, 13, 14}
29 The absence of a strong within-pair correlation in temporal tau BP_{ND} combined with the presence
30 of a strong within-pair correlation in temporal tau laterality quotient may indicate that genetic
31 factors influence the brain's regional vulnerability to tau pathology, but external factors (among

1 which amyloid- β , vascular components or lifestyle factors) that are unique to a twin may
2 influence the actual accumulation of tau. This is corroborated by our voxel-wise analyses,
3 indicating that the voxel-wise pattern of tau pathology was significantly more similar between
4 twins of the same pair compared to twins of random pairs, and that even though some twin pairs
5 were discordant for amyloid- β status, we could identify a twin solely based on the spatial
6 correlation with its co-twin in approximately 9 out of 10 pairs. The pathway through which
7 genetic factors may influence the regional localization of tau pathology remains to be further
8 examined, though recent *in vivo* PET studies support a role of brain connectivity patterns in the
9 spread of tau throughout the brain.^{13, 51-54} Whether the association between brain connectivity
10 and tau spread throughout the brain is influenced by shared underlying genetic mechanisms, for
11 example via the influence of genetics on cortical patterning and hub connectivity,^{55, 56} would be
12 of interest for future twin projects. Although the results of this study mainly reveal similarities in
13 tau PET characteristics in twin pairs, there were also twin pairs that showed strong dissimilarities
14 in tau PET of which two are highlighted in **Fig. 2**. A major question remains which factors can
15 explain the differences in tau pathology that we observed in twin pairs that are genetically
16 identical. Our data suggest that differences in amyloid- β pathology are likely associated with the
17 observed differences in tau, and this should be examined in more detail. We found that within-
18 pair differences in tau pathology were associated with within-pair differences in depressive
19 symptoms, social activity and physical activity. Interestingly, the observed associations between
20 within-pair differences in tau pathology and within-pair differences in depressive symptoms and
21 physical activity were partly independent of within-pair differences in global amyloid- β load.
22 Although unable to establish causality due to the cross-sectional design of the current study,
23 these findings are interesting given that previous studies have also linked resistance to
24 Alzheimer's disease pathology (lower levels of pathology than expected)⁵⁷ with lifestyle factors
25 including physical activity.^{58, 59} However, as the environmental risk factor variables in the
26 current study were measured at time of tau-PET, it is not possible to conclude whether these are
27 upstream or downstream effects of Alzheimer's disease pathology.

28 Future longitudinal twin studies will be of interest for several reasons. First, longitudinal
29 data may enable investigation of possible causal relationships between environmental (e.g.
30 lifestyle) risk factors, which may be potentially modifiable, Alzheimer's disease pathology and
31 cognitive decline. Second, longitudinal twin data is needed to clarify whether twins who are

1 currently different for Alzheimer's disease pathology (i.e. one twin having more pathology than
2 the co-twin), may over time become similar, or whether they remain different – and thus whether
3 it is a matter of a difference in disease development or a difference in the timing of disease onset.
4 Understanding which, potentially modifiable, environmental factors are associated with either
5 the complete absence or a delay in the onset and spread of tau pathology would be of great
6 importance for prevention strategies.

7 This study had some limitations. Firstly, we only included genetically identical twin
8 pairs, while classic twin studies include both genetically identical and fraternal twins, that share
9 on average half of their segregating genes. By not including fraternal twins, we could not
10 disentangle genetic from *shared* environmental influences. Secondly, our study was limited by a
11 relatively small sample size. Thirdly, a general limitation when studying preclinical Alzheimer's
12 disease pathology is that the overall levels of tau pathology are relatively low. Fourthly, second-
13 generation tau tracers may be preferred to examine tau pathology in the earliest stages of the
14 Alzheimer's disease continuum because of less off-target binding in the hippocampus, a region
15 in which tau accumulation occurs early in the disease process.^{8,9} Last, results are based on cross-
16 sectional data only, and longitudinal data will be needed to examine whether the within-pair
17 similarities may differ over time.

18 **Conclusion**

19 Our results indicate that genetically identical twins show substantial similarities in load, spatial
20 distribution and asymmetry measures of tau pathology, supportive of an important role for
21 genetic factors in the earliest stages of Alzheimer's disease. However, considering also the
22 presence of dissimilarities in tau pathology in twin pairs, genetics alone are likely insufficient to
23 explain the complete pathological course of the disease.

24 **Acknowledgements**

25 We kindly thank all participating twins for their dedication. Research of Amsterdam Alzheimer
26 Center is part of the Neurodegeneration program of Amsterdam Neuroscience. The Amsterdam
27 Alzheimer Center is supported by Alzheimer Nederland and Stichting VUmc funds.
28 [¹⁸F]Flortaucipir PET scans were made possible by Avid Radiopharmaceuticals Inc.

29

1 **Funding**

2 This study was made possible by the EU/European Federation of Pharmaceutical Industries and
3 Associations Innovative Medicines Initiative Joint Undertaking (EMIF grant 115372), the
4 European Grand Prix for Research of the Foundation on Alzheimer Disease and Alzheimer
5 Nederland 2016 and ZonMW Memorabel. This project has received funding from the Innovative
6 Medicines Initiative 2 Joint Undertaking under grant agreement No 115952. This Joint
7 Undertaking receives support from the European Union's Horizon 2020 research and innovation
8 program and EFPIA. This communication reflects the views of the authors and neither IMI nor
9 the European Union and EFPIA are liable for any use that may be made of the information
10 contained herein.

11 **Competing interests**

12 EMC, JT, RO, SSVG, MH, LEC, EW, SL, EEW, EJCG, AB report no competing interests.

13 ADW is editor-in-chief of Nuclear Medicine & Biology.

14 FB is supported by the NIHR UCLH biomedical research centre. FB is supported by the
15 European Union's Horizon 2020 research and innovation programme under grant agreement No.
16 666992.

17 PS has received consultancy fees (paid to the institution) from AC Immune, Biogen, Brainstorm
18 Cell, EIP, ImmunoBrain Checkpoint, Genentech, Novartis, Novo Nordisk. He is PI of studies
19 with AC Immune, CogRx, FUJI-film/Toyama, UCB, and Vivoryon. He is a part-time employee
20 of Life Sciences Partners Amsterdam. He serves on the board of Brain Research Center and New
21 Amsterdam Pharma.

22 PJV received nonfinancial support from GE Healthcare, research support from Biogen and grants
23 from EU/EFPIA Innovative Medicines Initiative Joint Undertaking, EU Joint Programme–
24 Neurodegenerative Disease Research (JPND and ZonMw).

25 BNMB received research support from ZonMW, AVID radiopharmaceuticals, CTMM and
26 Janssen Pharmaceuticals. He is a trainer for Piramal and GE. He receives no personal honoraria.

27

28 **Supplementary material**

29 Supplementary material is available at *Brain* online.

1 References

- 2 1. Sperling RA, Aisen PS, Beckett LA, et al. Toward defining the preclinical stages of Alzheimer's
3 disease: recommendations from the National Institute on Aging-Alzheimer's Association workgroups on
4 diagnostic guidelines for Alzheimer's disease. *Alzheimers Dement*. May 2011;7(3):280-92.
5 doi:10.1016/j.jalz.2011.03.003
- 6 2. Jansen WJ, Ossenkoppele R, Knol DL, et al. Prevalence of cerebral amyloid pathology in persons
7 without dementia: a meta-analysis. *JAMA*. May 19 2015;313(19):1924-38. doi:10.1001/jama.2015.4668
- 8 3. Jack CR, Jr., Holtzman DM. Biomarker modeling of Alzheimer's disease. *Neuron*. Dec 18
9 2013;80(6):1347-58. doi:10.1016/j.neuron.2013.12.003
- 10 4. Harrison TM, La Joie R, Maass A, et al. Longitudinal tau accumulation and atrophy in aging and
11 alzheimer disease. *Ann Neurol*. Feb 2019;85(2):229-240. doi:10.1002/ana.25406
- 12 5. Lehmann M, Ghosh PM, Madison C, et al. Diverging patterns of amyloid deposition and
13 hypometabolism in clinical variants of probable Alzheimer's disease. *Brain*. Mar 2013;136(Pt 3):844-58.
14 doi:10.1093/brain/aww327
- 15 6. Johnson KA, Schultz A, Betensky RA, et al. Tau positron emission tomographic imaging in aging
16 and early Alzheimer disease. *Ann Neurol*. Jan 2016;79(1):110-9. doi:10.1002/ana.24546
- 17 7. Vogel JW, Young AL, Oxtoby NP, et al. Four distinct trajectories of tau deposition identified in
18 Alzheimer's disease. *Nat Med*. Apr 29 2021;doi:10.1038/s41591-021-01309-6
- 19 8. Braak H, Braak E. Neuropathological staging of Alzheimer-related changes. *Acta Neuropathol*.
20 1991;82(4):239-59. doi:10.1007/BF00308809
- 21 9. Braak H, Braak E. Staging of Alzheimer's disease-related neurofibrillary changes. *Neurobiol Aging*.
22 May-Jun 1995;16(3):271-8; discussion 278-84. doi:10.1016/0197-4580(95)00021-6
- 23 10. Cho H, Choi JY, Hwang MS, et al. In vivo cortical spreading pattern of tau and amyloid in the
24 Alzheimer disease spectrum. *Ann Neurol*. Aug 2016;80(2):247-58. doi:10.1002/ana.24711
- 25 11. Scholl M, Lockhart SN, Schonhaut DR, et al. PET Imaging of Tau Deposition in the Aging Human
26 Brain. *Neuron*. Mar 2 2016;89(5):971-982. doi:10.1016/j.neuron.2016.01.028
- 27 12. Schwarz AJ, Yu P, Miller BB, et al. Regional profiles of the candidate tau PET ligand 18F-AV-1451
28 recapitulate key features of Braak histopathological stages. *Brain*. May 2016;139(Pt 5):1539-50.
29 doi:10.1093/brain/aww023
- 30 13. Vogel JW, Iturria-Medina Y, Strandberg OT, et al. Spread of pathological tau proteins through
31 communicating neurons in human Alzheimer's disease. *Nat Commun*. May 26 2020;11(1):2612.
32 doi:10.1038/s41467-020-15701-2
- 33 14. Ossenkoppele R, Schonhaut DR, Scholl M, et al. Tau PET patterns mirror clinical and
34 neuroanatomical variability in Alzheimer's disease. *Brain*. May 2016;139(Pt 5):1551-67.
35 doi:10.1093/brain/aww027
- 36 15. Hanseeuw BJ, Betensky RA, Jacobs HIL, et al. Association of Amyloid and Tau With Cognition in
37 Preclinical Alzheimer Disease: A Longitudinal Study. *JAMA Neurol*. Jun 3
38 2019;doi:10.1001/jamaneurol.2019.1424
- 39 16. Ossenkoppele R, Smith R, Ohlsson T, et al. Associations between tau, Abeta, and cortical
40 thickness with cognition in Alzheimer disease. *Neurology*. Feb 5 2019;92(6):e601-e612.
41 doi:10.1212/WNL.0000000000006875
- 42 17. Harrison TM, Du R, Klencklen G, Baker SL, Jagust WJ. Distinct effects of beta-amyloid and tau on
43 cortical thickness in cognitively healthy older adults. *Alzheimers Dement*. Dec 15
44 2020;doi:10.1002/alz.12249
- 45 18. Aschenbrenner AJ, Gordon BA, Benzinger TLS, Morris JC, Hassenstab JJ. Influence of tau PET,
46 amyloid PET, and hippocampal volume on cognition in Alzheimer disease. *Neurology*. Aug 28
47 2018;91(9):e859-e866. doi:10.1212/WNL.0000000000006075

- 1 19. Bejanin A, Schonhaut DR, La Joie R, et al. Tau pathology and neurodegeneration contribute to
2 cognitive impairment in Alzheimer's disease. *Brain*. Dec 1 2017;140(12):3286-3300.
3 doi:10.1093/brain/awx243
- 4 20. Visser D, Wolters EE, Verfaillie SCJ, et al. Tau pathology and relative cerebral blood flow are
5 independently associated with cognition in Alzheimer's disease. *Eur J Nucl Med Mol Imaging*. Dec
6 2020;47(13):3165-3175. doi:10.1007/s00259-020-04831-w
- 7 21. Maass A, Lockhart SN, Harrison TM, et al. Entorhinal Tau Pathology, Episodic Memory Decline,
8 and Neurodegeneration in Aging. *J Neurosci*. Jan 17 2018;38(3):530-543. doi:10.1523/JNEUROSCI.2028-
9 17.2017
- 10 22. Lowe VJ, Bruinsma TJ, Wiste HJ, et al. Cross-sectional associations of tau-PET signal with
11 cognition in cognitively unimpaired adults. *Neurology*. Jul 2 2019;93(1):e29-e39.
12 doi:10.1212/WNL.0000000000007728
- 13 23. Sperling RA, Mormino EC, Schultz AP, et al. The impact of amyloid-beta and tau on prospective
14 cognitive decline in older individuals. *Ann Neurol*. Feb 2019;85(2):181-193. doi:10.1002/ana.25395
- 15 24. Kremen WS, Prom-Wormley E, Panizzon MS, et al. Genetic and environmental influences on the
16 size of specific brain regions in midlife: the VETSA MRI study. *Neuroimage*. Jan 15 2010;49(2):1213-23.
17 doi:10.1016/j.neuroimage.2009.09.043
- 18 25. Posthuma D, de Geus EJ, Neale MC, et al. Multivariate genetic analysis of brain structure in an
19 extended twin design. *Behav Genet*. Jul 2000;30(4):311-9. doi:10.1023/a:1026501501434
- 20 26. Gatz M, Reynolds CA, Fratiglioni L, et al. Role of genes and environments for explaining
21 Alzheimer disease. *Arch Gen Psychiatry*. Feb 2006;63(2):168-74. doi:10.1001/archpsyc.63.2.168
- 22 27. Konijnenberg E, Carter SF, Ten Kate M, et al. The EMIF-AD PreclinAD study: study design and
23 baseline cohort overview. *Alzheimers Res Ther*. Aug 4 2018;10(1):75. doi:10.1186/s13195-018-0406-7
- 24 28. Collij LE, Konijnenberg E, Reimand J, et al. Assessing Amyloid Pathology in Cognitively Normal
25 Subjects Using (18)F-Flutemetamol PET: Comparing Visual Reads and Quantitative Methods. *J Nucl Med*.
26 Apr 2019;60(4):541-547. doi:10.2967/jnumed.118.211532
- 27 29. Collij LE, Heeman F, Salvado G, et al. Multitracer model for staging cortical amyloid deposition
28 using PET imaging. *Neurology*. Sep 15 2020;95(11):e1538-e1553. doi:10.1212/WNL.0000000000010256
- 29 30. Morris JC. The Clinical Dementia Rating (CDR): current version and scoring rules. *Neurology*. Nov
30 1993;43(11):2412-4. doi:10.1212/wnl.43.11.2412-a
- 31 31. Morris JC, Heyman A, Mohs RC, et al. The Consortium to Establish a Registry for Alzheimer's
32 Disease (CERAD). Part I. Clinical and neuropsychological assessment of Alzheimer's disease. *Neurology*.
33 Sep 1989;39(9):1159-65. doi:10.1212/wnl.39.9.1159
- 34 32. Yesavage JA, Brink TL, Rose TL, et al. Development and validation of a geriatric depression
35 screening scale: a preliminary report. *J Psychiatr Res*. 1982;17(1):37-49. doi:10.1016/0022-
36 3956(82)90033-4
- 37 33. Tuncel H, Visser D, Yaqub M, et al. Effect of Shortening the Scan Duration on Quantitative
38 Accuracy of [(18)F]Flortaucipir Studies. *Mol Imaging Biol*. Jan 26 2021;doi:10.1007/s11307-021-01581-5
- 39 34. Hammers A, Allom R, Koepp MJ, et al. Three-dimensional maximum probability atlas of the
40 human brain, with particular reference to the temporal lobe. *Hum Brain Mapp*. Aug 2003;19(4):224-47.
41 doi:10.1002/hbm.10123
- 42 35. Svarer C, Madsen K, Hasselbalch SG, et al. MR-based automatic delineation of volumes of
43 interest in human brain PET images using probability maps. *Neuroimage*. Feb 15 2005;24(4):969-79.
44 doi:10.1016/j.neuroimage.2004.10.017
- 45 36. Golla SS, Wolters EE, Timmers T, et al. Parametric methods for [(18)F]flortaucipir PET. *J Cereb*
46 *Blood Flow Metab*. Feb 2020;40(2):365-373. doi:10.1177/0271678X18820765

- 1 37. Golla SSV, Lubberink M, van Berckel BNM, Lammertsma AA, Boellaard R. Partial volume
2 correction of brain PET studies using iterative deconvolution in combination with HYPR denoising.
3 *EJNMMI Res.* Dec 2017;7(1):36. doi:10.1186/s13550-017-0284-1
- 4 38. Ossenkoppelle R, Rabinovici GD, Smith R, et al. Discriminative Accuracy of [18F]flortaucipir
5 Positron Emission Tomography for Alzheimer Disease vs Other Neurodegenerative Disorders. *JAMA.* Sep
6 18 2018;320(11):1151-1162. doi:10.1001/jama.2018.12917
- 7 39. Wolters EE, Golla SSV, Timmers T, et al. A novel partial volume correction method for accurate
8 quantification of [(18)F] flortaucipir in the hippocampus. *EJNMMI Res.* Aug 15 2018;8(1):79.
9 doi:10.1186/s13550-018-0432-2
- 10 40. Oldfield RC. The assessment and analysis of handedness: the Edinburgh inventory.
11 *Neuropsychologia.* Mar 1971;9(1):97-113. doi:10.1016/0028-3932(71)90067-4
- 12 41. Konijnenberg E, Tomassen J, den Braber A, et al. Onset of Preclinical Alzheimer Disease in
13 Monozygotic Twins. *Ann Neurol.* Feb 14 2021;doi:10.1002/ana.26048
- 14 42. Livingston G, Huntley J, Sommerlad A, et al. Dementia prevention, intervention, and care: 2020
15 report of the Lancet Commission. *Lancet.* Aug 8 2020;396(10248):413-446. doi:10.1016/S0140-
16 6736(20)30367-6
- 17 43. Smits C, Theo Goverts S, Festen JM. The digits-in-noise test: assessing auditory speech
18 recognition abilities in noise. *J Acoust Soc Am.* Mar 2013;133(3):1693-706. doi:10.1121/1.4789933
- 19 44. Washburn RA, Smith KW, Jette AM, Janney CA. The Physical Activity Scale for the Elderly (PASE):
20 development and evaluation. *J Clin Epidemiol.* Feb 1993;46(2):153-62. doi:10.1016/0895-4356(93)90053-
21 4
- 22 45. Baker SL, Harrison TM, Maass A, La Joie R, Jagust WJ. Effect of Off-Target Binding on (18)F-
23 Flortaucipir Variability in Healthy Controls Across the Life Span. *J Nucl Med.* Oct 2019;60(10):1444-1451.
24 doi:10.2967/jnumed.118.224113
- 25 46. De Moor MH, Boomsma DI, Stubbe JH, Willemsen G, de Geus EJ. Testing causality in the
26 association between regular exercise and symptoms of anxiety and depression. *Arch Gen Psychiatry.* Aug
27 2008;65(8):897-905. doi:10.1001/archpsyc.65.8.897
- 28 47. Brickell KL, Leverenz JB, Steinbart EJ, et al. Clinicopathological concordance and discordance in
29 three monozygotic twin pairs with familial Alzheimer's disease. *J Neurol Neurosurg Psychiatry.* Oct
30 2007;78(10):1050-5. doi:10.1136/jnnp.2006.113803
- 31 48. Iacono D, Volkman I, Nennesmo I, et al. Neuropathologic assessment of dementia markers in
32 identical and fraternal twins. *Brain Pathol.* Jul 2014;24(4):317-33. doi:10.1111/bpa.12127
- 33 49. Bennett RE, DeVos SL, Dujardin S, et al. Enhanced Tau Aggregation in the Presence of Amyloid
34 beta. *Am J Pathol.* Jul 2017;187(7):1601-1612. doi:10.1016/j.ajpath.2017.03.011
- 35 50. Wolters EE, Ossenkoppelle R, Verfaillie SCJ, et al. Regional [(18)F]flortaucipir PET is more closely
36 associated with disease severity than CSF p-tau in Alzheimer's disease. *Eur J Nucl Med Mol Imaging.* Nov
37 2020;47(12):2866-2878. doi:10.1007/s00259-020-04758-2
- 38 51. Ossenkoppelle R, Iaccarino L, Schonhaut DR, et al. Tau covariance patterns in Alzheimer's disease
39 patients match intrinsic connectivity networks in the healthy brain. *Neuroimage Clin.* 2019;23:101848.
40 doi:10.1016/j.nicl.2019.101848
- 41 52. Cope TE, Rittman T, Borchert RJ, et al. Tau burden and the functional connectome in Alzheimer's
42 disease and progressive supranuclear palsy. *Brain.* Feb 1 2018;141(2):550-567.
43 doi:10.1093/brain/awx347
- 44 53. Franzmeier N, Rubinski A, Neitzel J, et al. Functional connectivity associated with tau levels in
45 ageing, Alzheimer's, and small vessel disease. *Brain.* Apr 1 2019;142(4):1093-1107.
46 doi:10.1093/brain/awz026

- 1 54. Jacobs HL, Hedden T, Schultz AP, et al. Structural tract alterations predict downstream tau
 2 accumulation in amyloid-positive older individuals. *Nat Neurosci.* Mar 2018;21(3):424-431.
 3 doi:10.1038/s41593-018-0070-z
- 4 55. Schmitt JE, Neale MC, Fassassi B, et al. The dynamic role of genetics on cortical patterning during
 5 childhood and adolescence. *Proc Natl Acad Sci U S A.* May 6 2014;111(18):6774-9.
 6 doi:10.1073/pnas.1311630111
- 7 56. Arnatkeviciute A, Fulcher BD, Oldham S, et al. Genetic influences on hub connectivity of the
 8 human connectome. *Nat Commun.* Jul 9 2021;12(1):4237. doi:10.1038/s41467-021-24306-2
- 9 57. Arenaza-Urquijo EM, Vemuri P. Resistance vs resilience to Alzheimer disease: Clarifying
 10 terminology for preclinical studies. *Neurology.* Apr 10 2018;90(15):695-703.
 11 doi:10.1212/WNL.0000000000005303
- 12 58. Okonkwo OC, Schultz SA, Oh JM, et al. Physical activity attenuates age-related biomarker
 13 alterations in preclinical AD. *Neurology.* Nov 4 2014;83(19):1753-60.
 14 doi:10.1212/WNL.0000000000000964
- 15 59. Schreiber S, Vogel J, Schwimmer HD, Marks SM, Schreiber F, Jagust W. Impact of lifestyle
 16 dimensions on brain pathology and cognition. *Neurobiol Aging.* Apr 2016;40:164-172.
 17 doi:10.1016/j.neurobiolaging.2016.01.012

18

19 **Figure Legends**

20 **Figure 1 Group-average image of [¹⁸F]flortaucipir BP_{ND}.**

21 **Figure 2 Examples of [¹⁸F]flortaucipir PET scans from six genetically identical twin pairs.**

22 Shown are the [¹⁸F]flortaucipir PET scans from six genetically identical twin pairs. For
 23 illustration purposes, we selected pairs that show within-pair similarities in [¹⁸F]flortaucipir BP_{ND}
 24 and distribution (top and middle row), as well as within-pair dissimilarities (bottom row).

25 **Figure 3 Identical twin pair correlations for global and regional [¹⁸F]flortaucipir BP_{ND}.**

26 (A) For each ROI, we performed age- and sex-adjusted one-way single-measure intra-class
 27 correlations across twin pairs (i.e. a correlation between Twin 1 and Twin 2 across the group) to
 28 examine within-pair similarities in [¹⁸F]flortaucipir BP_{ND} (tau load); (B) Scatterplots illustrating
 29 twin-pair correlations in [¹⁸F]flortaucipir BP_{ND} for each ROI. Each dot represents a twin-pair.
 30 The values presented in the plots are the residuals of [¹⁸F]flortaucipir BP_{ND} in Twin 1 (y-axis)
 31 and Twin 2 (x-axis) after regressing out the effects of age and sex. (C) The correlation coefficient
 32 observed for twin pairs (see panel B) is plotted against the distribution of correlation coefficients
 33 observed for random pairs. * $p < 0.05$; ** $p < 0.01$

34

35 **Figure 4 Identical twin pair correlations for hemispheric lateralization in global and**

36 **regional [¹⁸F]flortaucipir BP_{ND}.** Shown are the scatterplots illustrating the twin-pair

1 associations in regional laterality quotients for [^{18}F]flortaucipir BP_{ND} . Each dot represents a twin-
 2 pair. The values presented in the plots are the residuals of the laterality quotient in regional and
 3 global [^{18}F]flortaucipir BP_{ND} for Twin 1 (y-axis) and Twin 2 (x-axis) after regressing out the
 4 effects of age and sex. * $p < 0.05$; ** $p < 0.01$

5 **Figure 5 Spatial correlations for [^{18}F]flortaucipir PET between each participant and every**
 6 **other participant. (A)** We correlated each participant's voxel-by-voxel [^{18}F]flortaucipir spatial
 7 distribution to that of every other participant using Spearman correlation models; **(B)** The
 8 distribution of spatial correlations (spearman's rho coefficient, corrected for age and sex)
 9 observed for twin pairs is compared against the distribution of spatial correlations observed for
 10 non-twin pairs.

11 **Figure 6 Within twin-pair differences regression models between within-pair differences in**
 12 **[^{18}F]flortaucipir BP_{ND} and within-pair differences in GDS total score, social activity and**
 13 **PASE total score.**

14 Each dot represents a twin-pair. Values presented in the plots represent the raw difference in
 15 temporal [^{18}F]flortaucipir BP_{ND} between Twin 1 and Twin 2 for each pair (y-axis), and the raw
 16 differences in GDS total score, social activity and PASE total score between Twin 1 and Twin 2
 17 for each pair (x-axis). Reported β and p values are from age- and sex-corrected regression
 18 models. * $p < 0.05$

19
 20 **Table 1 Demographics**

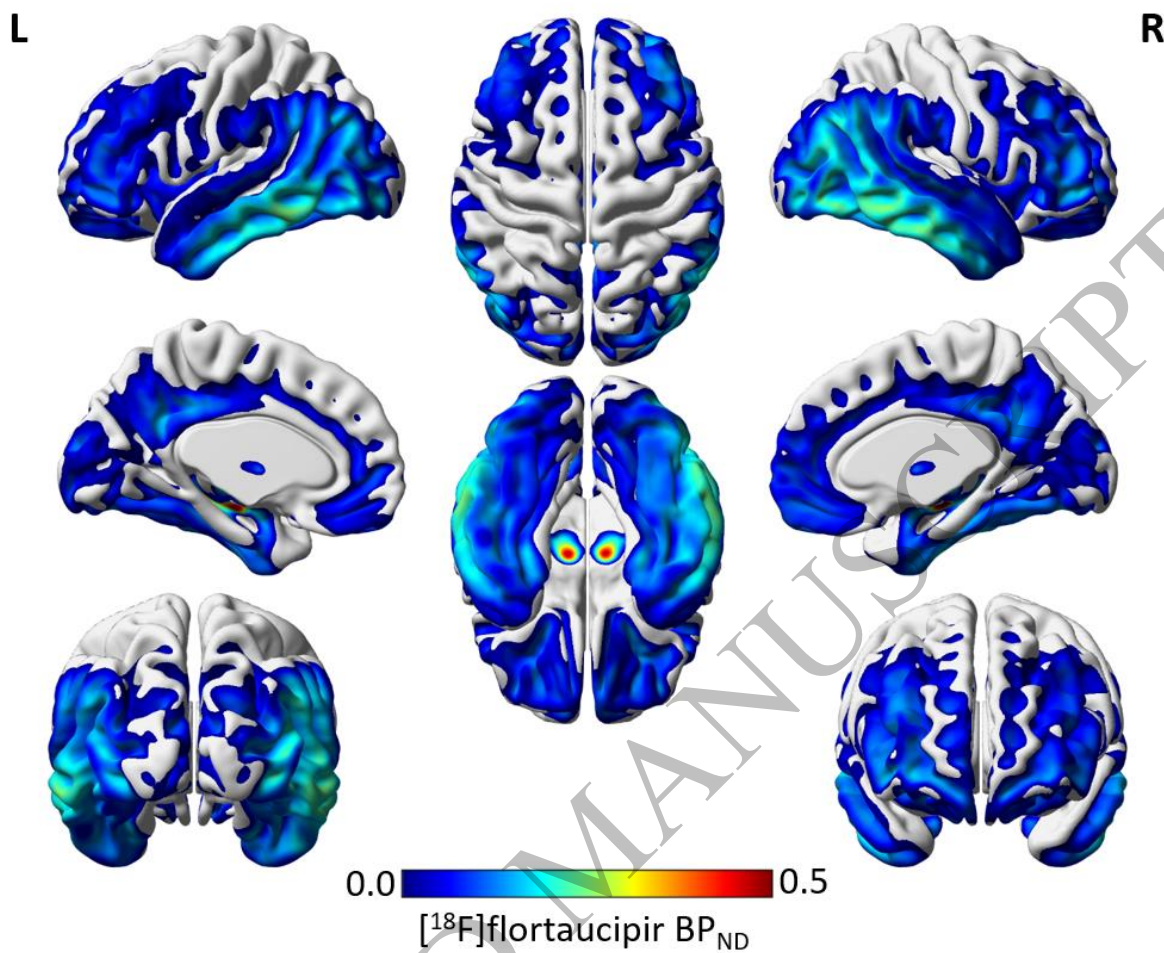
	Total sample
N	78 (39 pairs)
Age, y	73.4 \pm 5.9
Female, n (%)	40 (51.3%)
Education, y	12.3 \pm 2.9
MMSE score	28.7 \pm 1.3
APOE ϵ 4 positivity, n (%)	40 (51.3%)
Amyloid- β status, n positive (%)	15 (19.2%)
Amyloid- β twin-pair status, n pairs	
Amyloid- β concordant negative	28 pairs
Amyloid- β discordant	7 pairs
Amyloid- β concordant positive	4 pairs
Global [^{18}F]flutemetamol BP_{ND}	0.18 \pm 0.14 ^a
[^{18}F]flortaucipir BP_{ND}	
Entorhinal (Braak I)	0.02 \pm 0.14
Temporal (Braak III-IV)	0.10 \pm 0.08

Neocortical (Braak V-VI)	0.04 ± 0.05
Global (Braak I-VI)	0.04 ± 0.05

1 Mean ± SD are reported unless stated otherwise. Age and MMSE are measured at time of tau-PET; amyloid- β variables are from 4 years prior
2 to tau-PET.

3 ^aGlobal [¹⁸F]flutemetamol BP_{ND} was missing for 4 participants.
4
5
6
7
8
9
10
11
12
13
14

ACCEPTED MANUSCRIPT



0.0  0.5
[¹⁸F]flortaucipir BP_{ND}

Figure 1
160x131 mm (.80 x DPI)

1
2
3
4

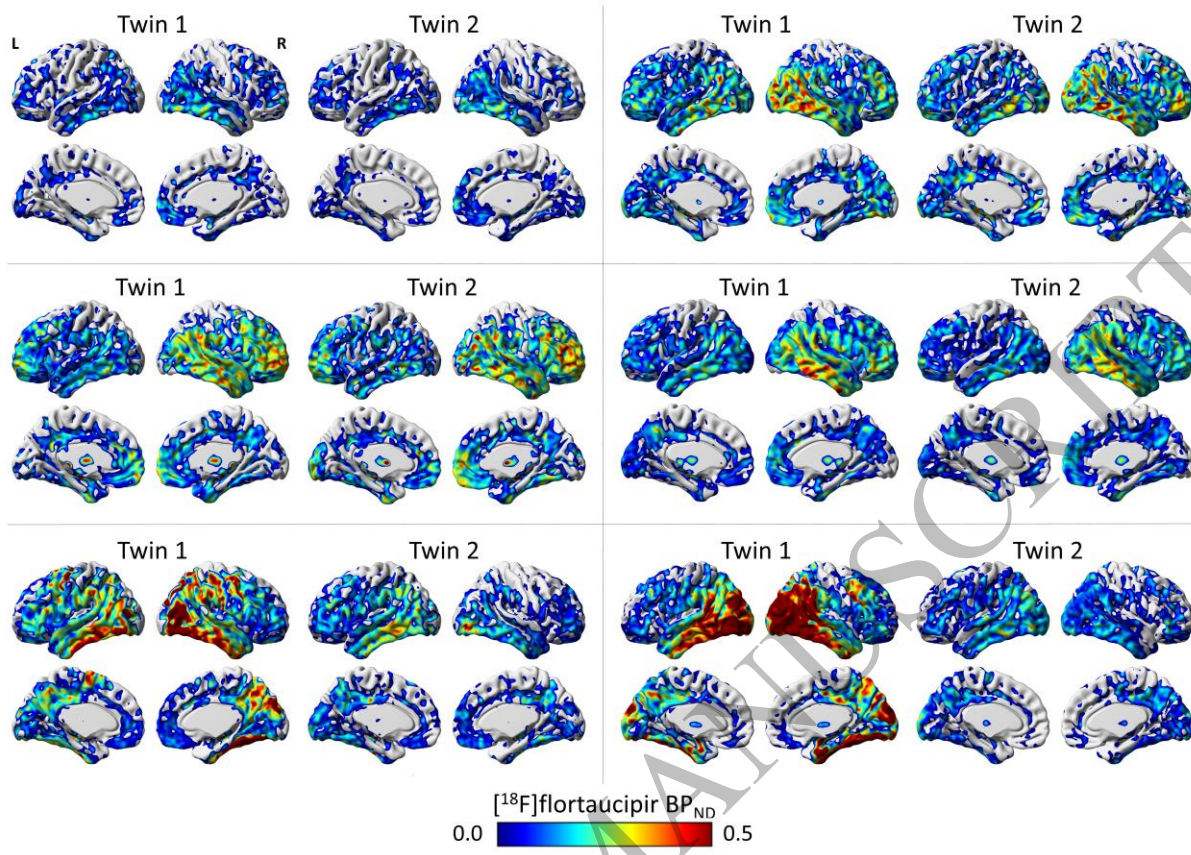


Figure 2
160x114 mm (.80 x DPI)

1
2
3
4

ACCEPTED

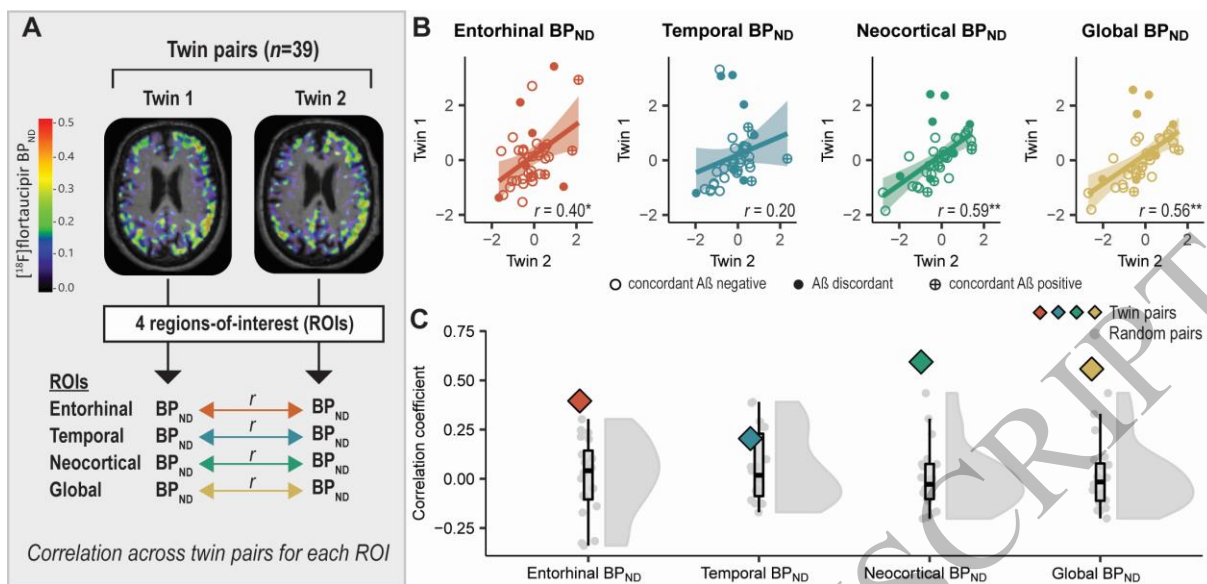


Figure 3
160x76 mm (.80 x DPI)

1
2
3
4

ACCEPTED MANUSCRIPT

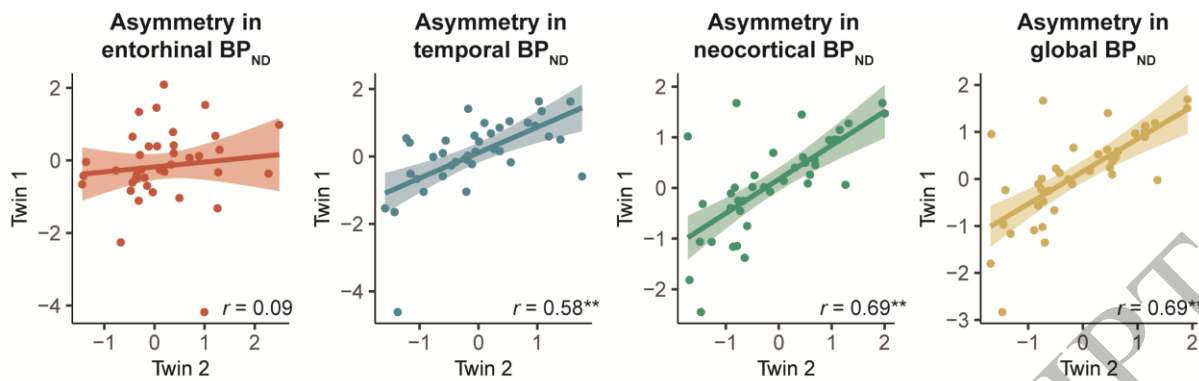


Figure 4
160x51 mm (.80 x DPI)

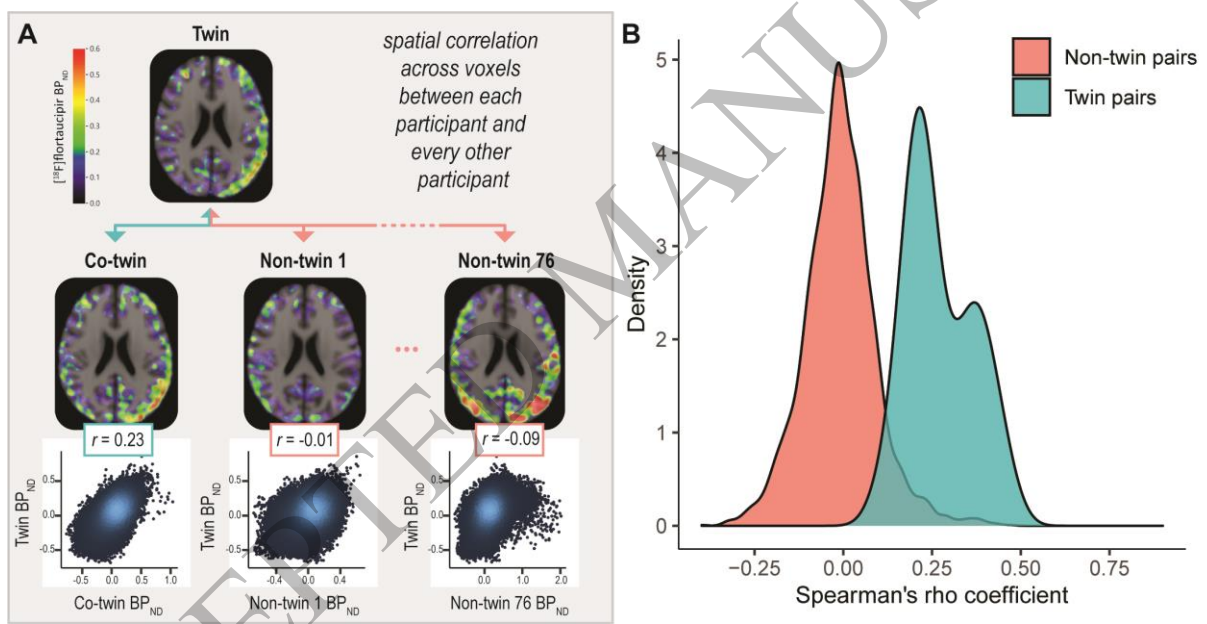


Figure 5
160x81 mm (.80 x DPI)

1
2
3
4
5

6
7
8
9

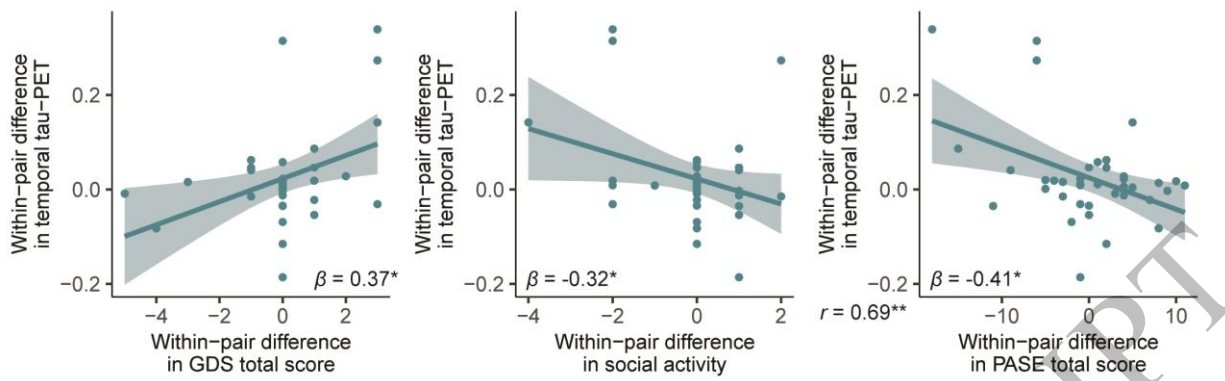


Figure 6
160x52 mm (.80 x DPI)

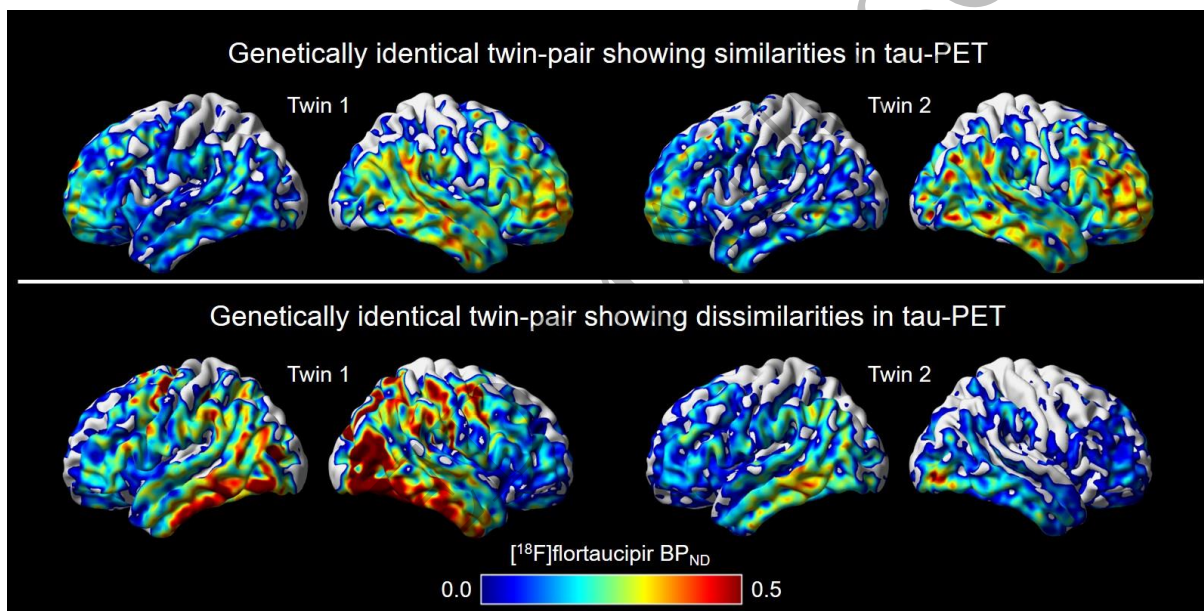


Figure 7
160x80 mm (.80 x DPI)

1
2
3
4

5
6
7
8

1 Coomans *et al.* reveal substantial similarities in tau load and spatial distribution in identical twins,
2 and show that they can identify pairs of twins based on tau spatial distribution. However, within-
3 pair differences – particularly in tau load – also suggest a role for (modifiable) environmental
4 factors in tau accumulation.
5

ACCEPTED MANUSCRIPT